In Silico Fight Against Novel Coronavirus by Finding Chromone Derivatives as Inhibitor of Coronavirus Main Proteases Enzyme

Nayim Sepay[a]*, Nadir Sepay[b], Ashique Al Hoque[c], Rina Mondal[d], Umesh Chandra Halder[a]* and Mohd. Muddassir[e]

[a]Department of Chemistry, Jadavpur University, Kolkata 700032, India.

[b]Plant Biotechnology Laboratory, Post Graduate Department of Botany, Ramakrishna Mission Vivekananda Centenary College, Rahara, Kolkata -700118, India.

[c]Department of Pharmaceutical Technology, Jadavpur University, Kolkata 700032, India.

[d]Department of Chemistry, Uluberia College, Howrah, West Bengal 711 315, India.

[e]Department of Chemistry, College of Science, King Saud University, Riyadh 11451, Saudi Arabia.

*Corresponding authors

Email: nayimsepay@yahoo.com (NS) and uhalder2002@yahoo.com (UCH)

Methods

The study focused on the mutant and earlier three CoV M^{pro}, i.e. 6lu7, 2q6d, 2q6f and 2h2z, respectively, for in silico finding of having the capacity to develop into inhibitors in the near future from chromanone derivatives.

Protein structure modelling.
The crystal data of all the protein structures were downloaded from Protein Data Bank (PDB ID: 6lu7, 2q6d, 2q6f and 2h2z). The structures used for further studies was prepared by Discovery studio 2017 R2 client. The modelling of protein structure was done on I-TASSER. All the pictures of the protein was made with MolSoft-ICM browser, Discovery studio 2017 R2 client and Samson core software.

Bioinformatics.
The protein sequences of selected four above mentioned proteins have been obtained from Discovery studio 2017 R2 client. The sequences were aligned using the bioinformatics web server Clustal Omega of European Bioinformatics Institute (EMBL-EBI). The outcome of the alignment protein sequences was analysed in the same web server, m-view and visualised it with the colour coding provided by the server.

Molecular Electrostatic Potential (MEP) Analysis
The compounds **2a-j** were optimized with the help of density functional theory using B3LYP functional at 6-311g level of besis set. Molecular electrostatic potential map around the molecular frame work were calculated at the combined B3LYP and 6-31g level of theory with the 0.03 iso values. For all of these DFT calculations, Gaussian 09W software with D1 revision has been used at windows platform [1].

ADME study
ADME and toxicity of the designed compounds were predicted at the SwissADME web server [2]. Using huge database, the server can speculate physicochemical properties, lipophilicity, water solubility, pharmacokinetics, drug likeness and medicinal properties with high precision.

Molecular docking estimation
Energy minimized structure of compounds **2a-j**, obtained from DFT optimization and were used for docking with the mentioned four protein structures. The structure of the compounds and proteins were prepared in appropriate format for the studies with the help of MGL Tools. For docking studies, AutoDock 4.2 was employed by following standard procedure as described.[3] In this case, a 40 x 40 x 40 grid box has been used [3].

Toxicity
Cardiac Toxicity of all the compounds (2a-2j) have been predicted with the help of a web-accessible computational equipment Pred-hERG [4]. Acute toxicity, organ toxicity, toxicological endpoint, nuclear receptor signalling pathways and stress response pathway was also calculated for these compounds and some FDA approved anti-viral drugs using PROTOX-II [5].

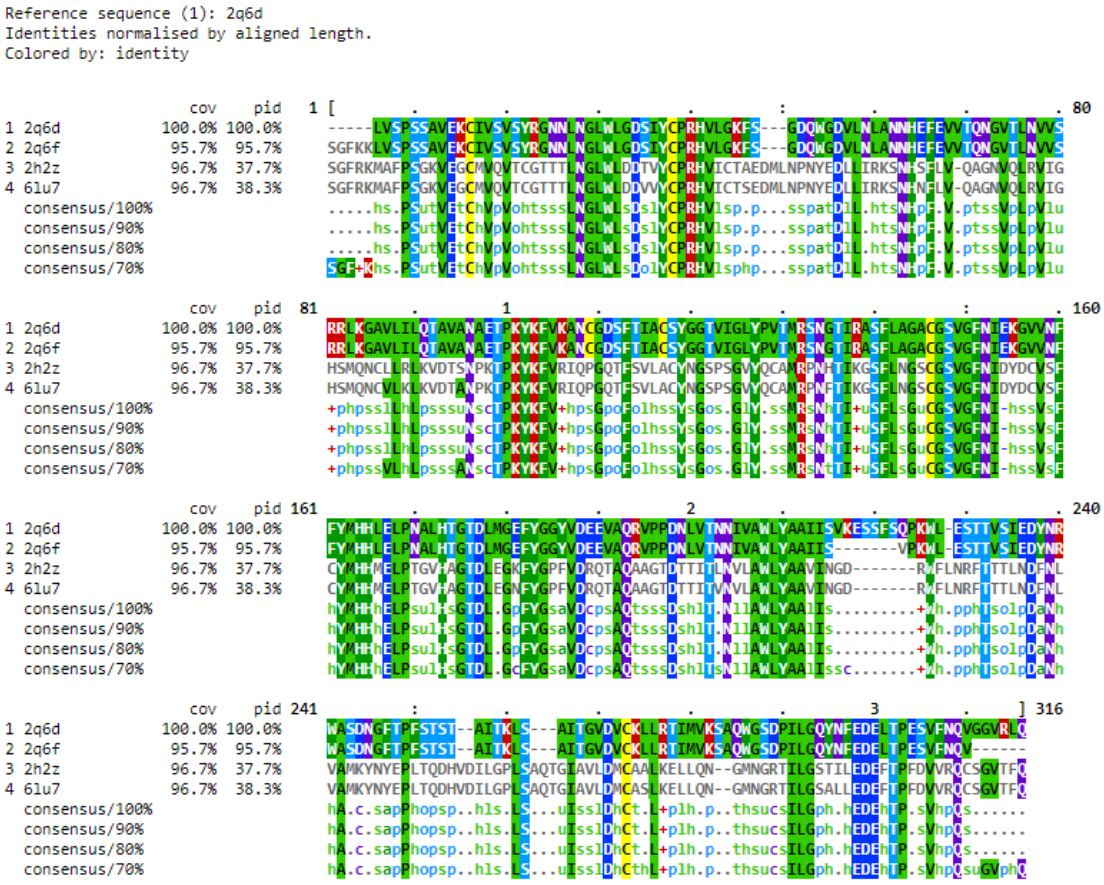

Figure S1: MView representation of protein sequence alignment of novel and previously known CoV M^{pro} (pdb ids: 6lu7, 2q6d, 2q6f and 2h2z)

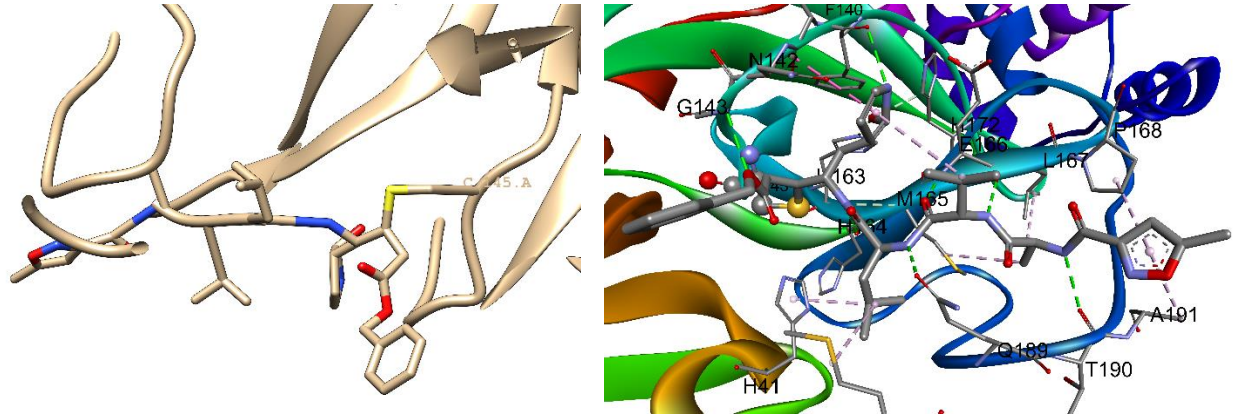

(a) (b)

Figure S2: **(a) Binding of N3 liganCovalent** Amino acid residue at the active site of the mutant coronavirus main protease (SARC-CoV-2 M^{pro}) (pdb id 6lu7).

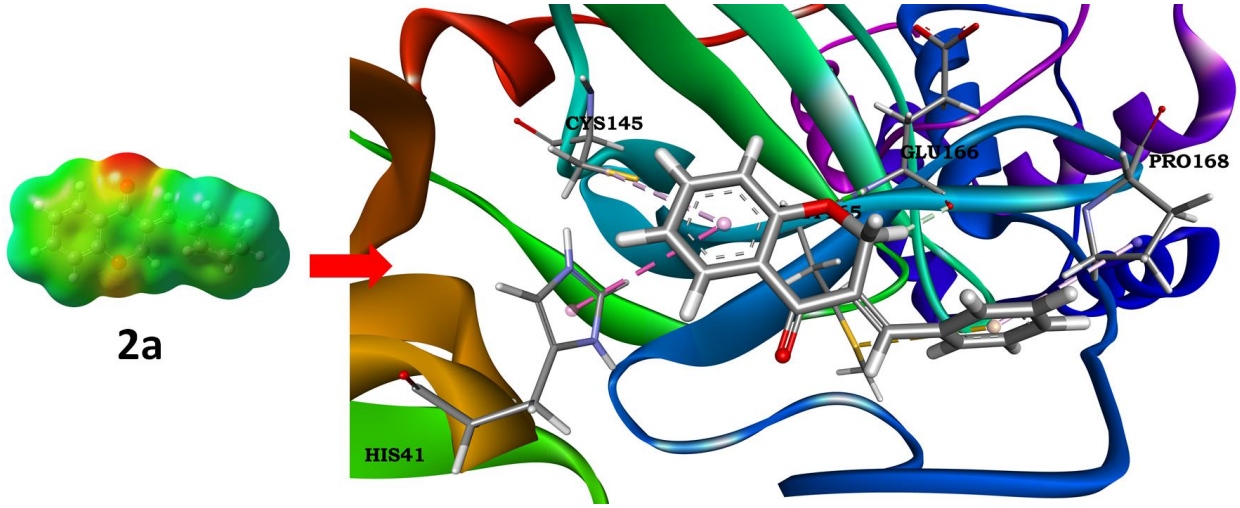

Figure S3: Docking pose of compound **2a** with SARC-CoV-2 M^{pro} of novel corona virus and the non-covalent interactions causes for their binding.

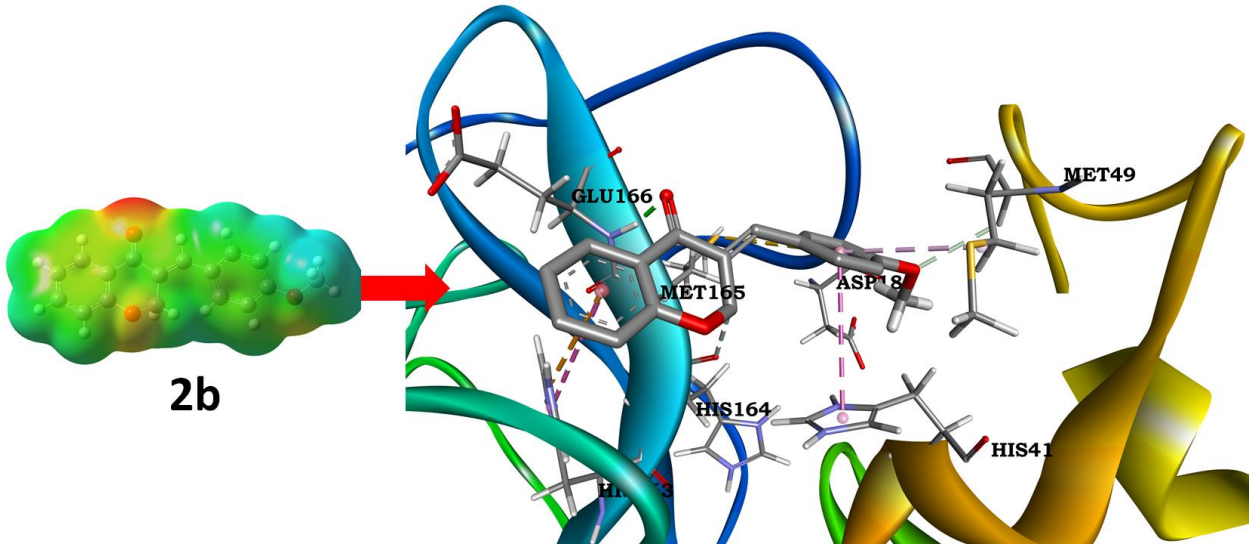

Figure S4: Docking pose of compound **2b** with SARC-CoV-2 M^{pro} of novel corona virus and the non-covalent interactions causes for their binding.

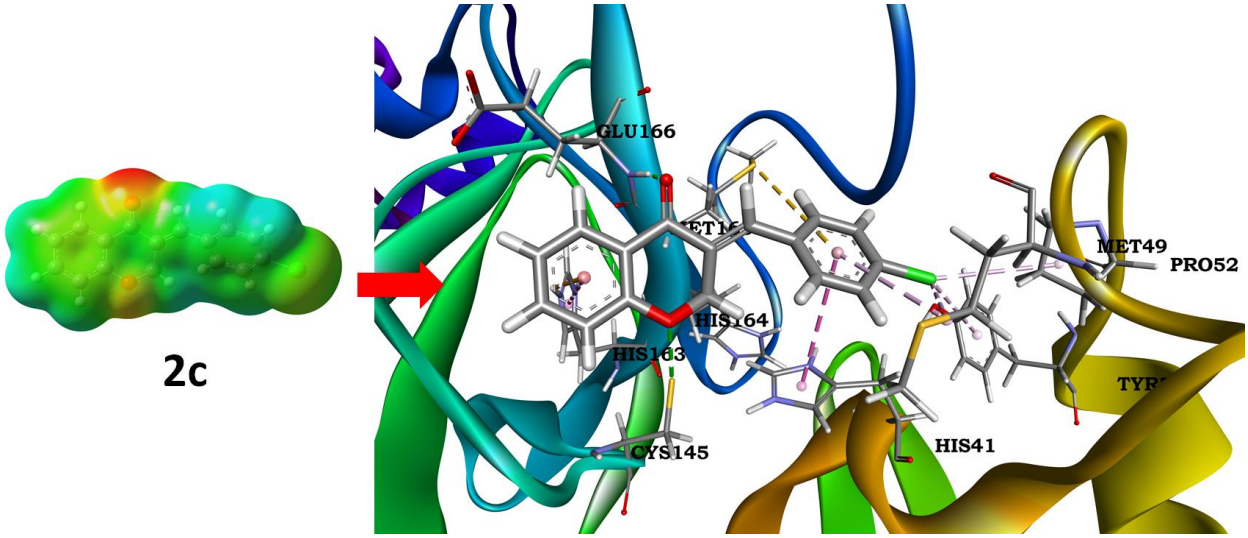

Figure S5: Docking pose of compound **2c** with SARC-CoV-2 M^{pro} of novel corona virus and the non-covalent interactions causes for their binding.

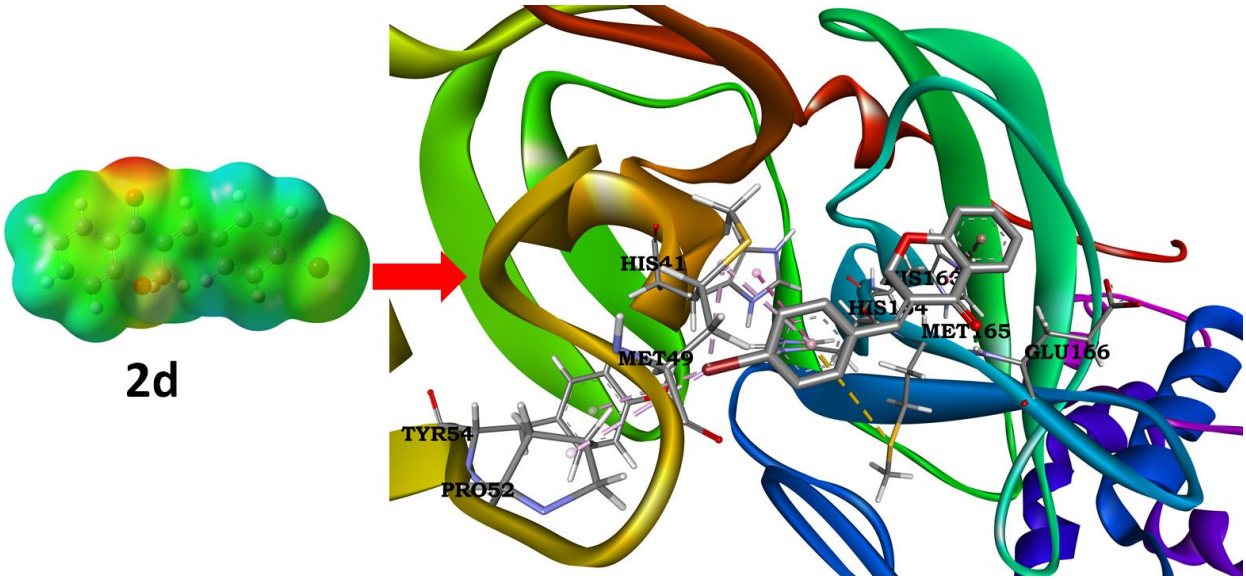

Figure S6: Docking pose of compound **2d** with SARC-CoV-2 M^{pro} of novel corona virus and the non-covalent interactions causes for their binding.

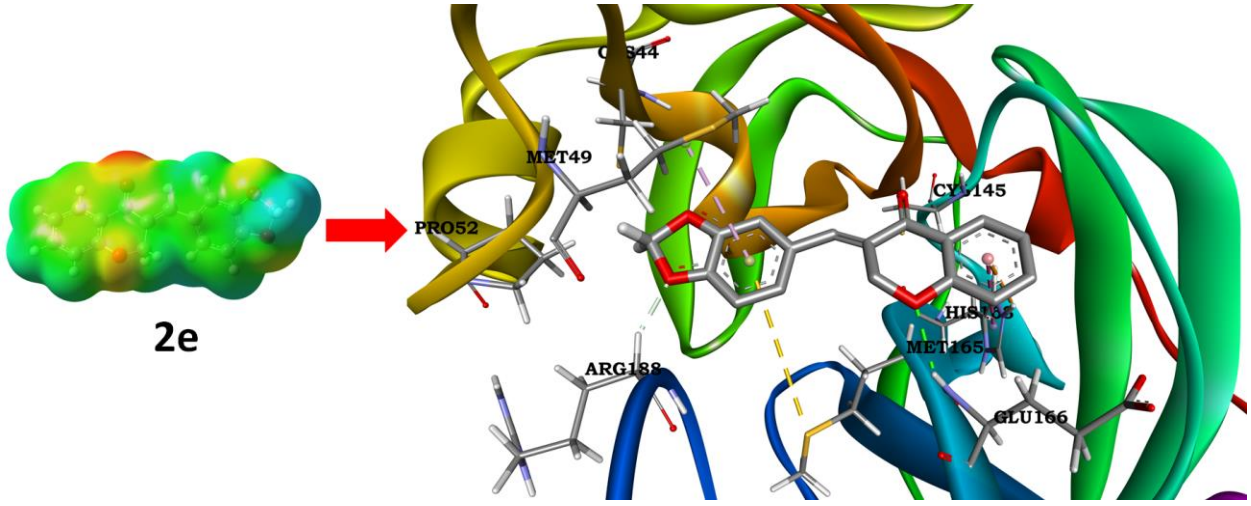

Figure S7: Docking pose of compound **2e** with SARC-CoV-2 M^{pro} of novel corona virus and the non-covalent interactions causes for their binding.

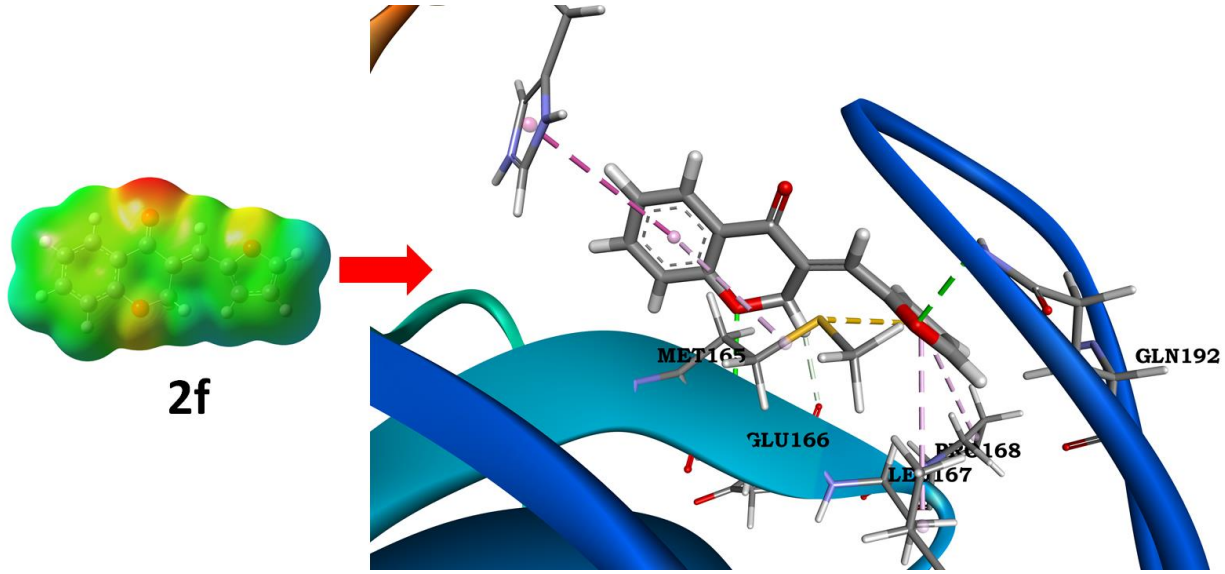

Figure S8: Docking pose of compound **2f** with SARC-CoV-2 M^{pro} of novel corona virus and the non-covalent interactions causes for their binding.

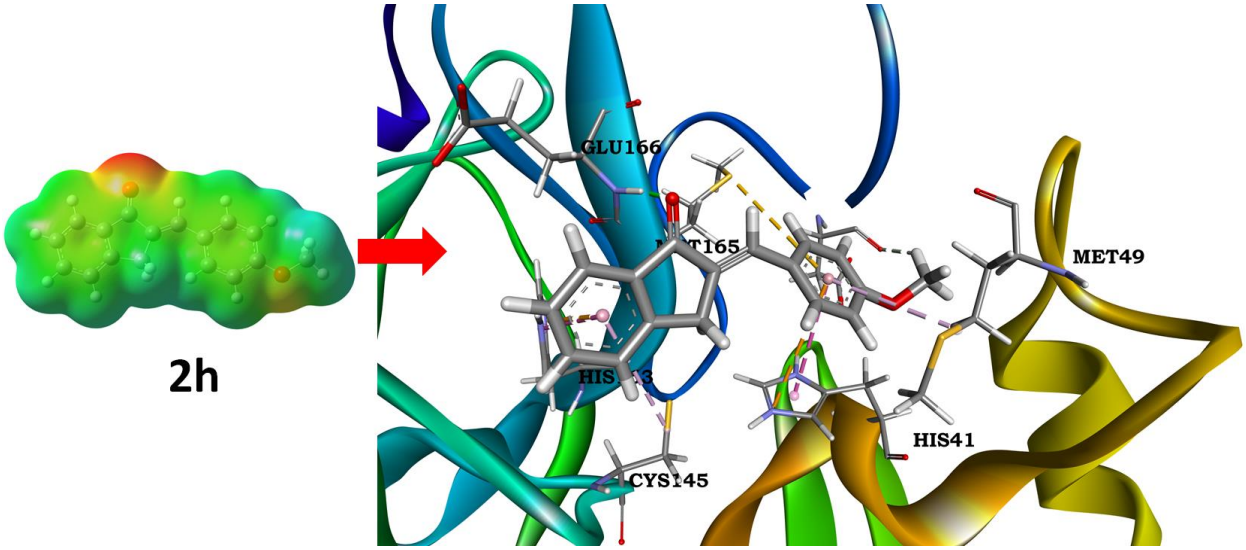

Figure S9: Docking pose of compound **2h** with SARC-CoV-2 M^{pro} of novel corona virus and the non-covalent interactions causes for their binding.

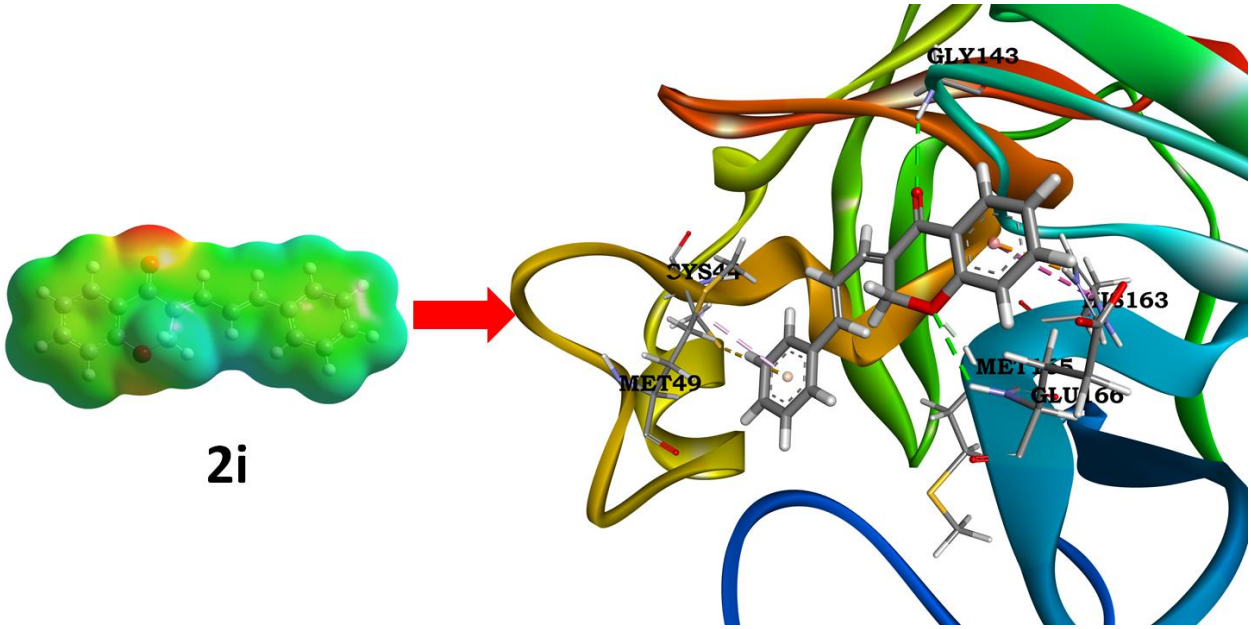

Figure S10: Docking pose of compound **2i** with SARC-CoV-2 M^{pro} of novel corona virus and the non-covalent interactions causes for their binding.

Table S1 Protein inhibitory activity of some flavones and 3-benzylidene-4-chromanones

Entry	Compound	Inhibitory Activity	Reference
1	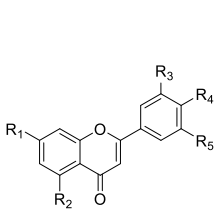	Acetylcholinesterase	*Med Chem Res.* **2018**, *27*, 520–530,
2	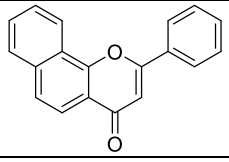	microsomal cytochrome P450	*J.Biol.Chem.* **2007**, *282*, 14348-14355
3	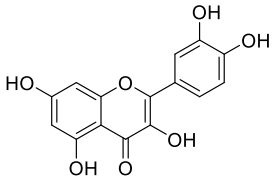	1. Xanthine oxidase inhibition 2. PDE4 inhibition	1. *Arch. Biochem. Biophys*. **2008**, *469*, 209–219 2. *Invest. New Drugs* **2008**, *26*, 417–424 *Biochem. Pharmacol*. **2004**, *68*, 2087–2094
4	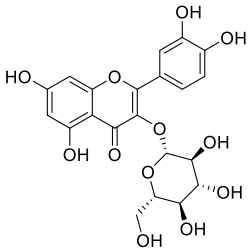	1. NADPH oxidase inhibition 2. Xanthine oxidase inhibition	1. *Arch. Biochem. Biophys*. **2008**, *469*, 209–219 2. *Trends Pharmacol Sc* **2012**, *33*, 602-610
5	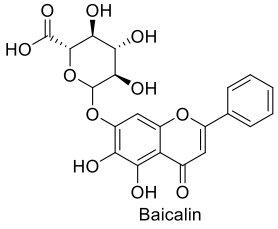	1. Xanthine oxidase inhibition 2. PDE4 inhibition	1. *Arch. Biochem. Biophys*. **2008**, *469*, 209–219 2. *Invest. New Drugs* **2008**, *26*, 417–424 3. *Biochem. Pharmacol*. **2004**, *68*, 2087–2094
6	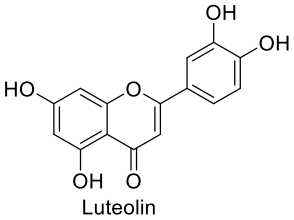	1. Xanthine oxidase inhibition 2. PDE4 inhibition	1. *Arch. Biochem. Biophys*. **2008**, *469*, 209–219 2. *Invest. New Drugs* **2008**, *26*, 417–424 3. *Biochem. Pharmacol*. **2004**, *68*, 2087–2094

7	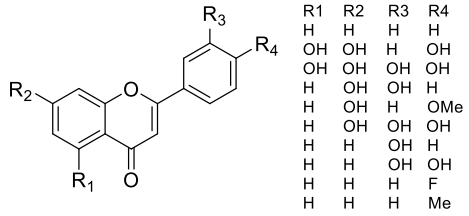	Tankyrases-2	*J. Med. Chem.* **2013**, *56*, 3507-3517
8	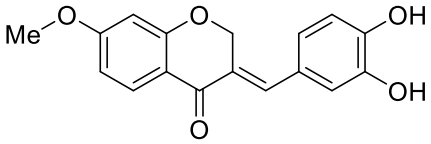	α-glucosidase inhibitory	*Chem. Pharm. Bull*. **2016**, *64*, 1203−1207.
9	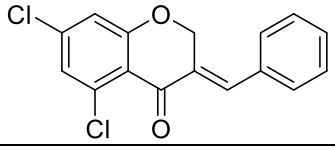	MAO-B inhibitor	*Eur. J. Med. Chem*. **2016**, *117*, 292−300.
10	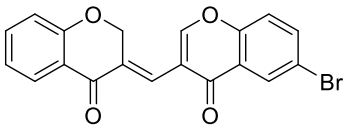	AChE inhibitors	*J. Photochem. Photobiol.,B* **2014**, *130*, 179−187.
11	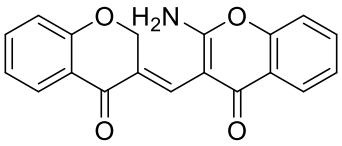	AChE inhibitors	*J. Photochem. Photobiol.,B* **2014**, *130*, 179−187.

Table S2 Predicted data of lipophilicity of the designed compound by different methods.

Molecule	iLOGP	XLOGP3	WLOGP	MLOGP	Silicos-IT Log P
2a	2.69	3.33	3.24	2.64	4.02
2b	3.00	3.31	3.25	2.27	4.03
2c	2.92	3.96	3.89	3.15	4.63
2d	3.06	4.03	4.00	3.27	4.67
2e	2.94	3.15	2.97	2.09	3.88
2f	2.44	2.43	2.83	1.29	3.41
2g	2.88	4.5	4.6	4.08	5.19
2h	2.72	3.76	3.41	2.88	4.42
2i	3.03	3.98	3.79	3.04	4.57
2j	1.49	2.48	2.95	1.71	2.84

Table S3: Predicted data of water solubility of the designed compound by different methods.

	2a	**2b**	**2c**	**2d**	**2e**	**2f**	**2g**	**2h**	**2i**	**2j**
ESOL LogS	-3.83	-3.89	-4.41	-4.73	-3.92	-3.19	-4.85	-4.1	-4.29	-3.62
ESOL Solubility (mg/ml)	3.49E-02	3.44E-02	1.04E-02	5.81E-03	3.38E-02	1.47E-01	4.01E-03	2.01E-02	1.36E-02	7.26E-02
ESOL Solubility (mol/l)	1.48E-04	1.29E-04	3.85E-05	1.84E-05	1.20E-04	6.51E-04	1.40E-05	8.02E-05	5.18E-05	2.43E-04
ESOL Class	Soluble	Soluble	Mod. solu*	Mod. solu	Soluble	Soluble	Mod. solu	Mod. solu	Mod. solu	Soluble
Ali Log S	-3.56	-3.73	-4.21	-4.29	-3.76	-2.90	-5.11	-4.01	-4.23	-4.41
Ali Solubility (mg/ml)	6.52E-02	4.93E-02	1.66E-02	1.63E-02	4.87E-02	2.84E-01	2.22E-03	2.47E-02	1.53E-02	1.16E-02
Ali Solubility (mol/l)	2.76E-04	1.85E-04	6.13E-05	5.18E-05	1.74E-04	1.26E-03	7.75E-06	9.88E-05	5.84E-05	3.89E-05
Ali Class	Soluble	Soluble	Mod. solu	Mod. solu	Soluble	Soluble	Mod. solu	Mod. solu	Mod. solu	Mod. solu
Silicos-IT LogSw	-5.41	-5.53	-6.02	-6.24	-5.15	-4.62	-6.38	-5.8	-5.5	-4.25
Silicos-IT Solubility (mg/ml)	9.19E-04	7.80E-04	2.59E-04	1.83E-04	1.97E-03	5.36E-03	1.18E-04	4.00E-04	8.37E-04	1.66E-02
Silicos-IT Solubility (mol/l)	3.89E-06	2.93E-06	9.55E-07	5.79E-07	7.01E-06	2.37E-05	4.13E-07	1.60E-06	3.19E-06	5.56E-05
Silicos-IT class	Mod. solu	Mod. solu	Poor solu	Poor solu	Mod. solu	Mod. solu	Poor solu	Mod. solu	Mod. solu	Mod. solu

*Mod. solu = Moderately soluble

Table S4: Predicted data of pharmacokinetics, drug likeness and medicinal chemistry of the designed compound

	2a	**2b**	**2c**	**2d**	**2e**	**2f**	**2g**	**2h**	**2i**	**2j**
GI absorption	High	High	High	High	High	High	High	High	High	High
BBB permeant	Yes	Yes	Yes	Yes	Yes	Yes	Yes	Yes	Yes	No
Pgp substrate	No	No	No	No	No	No	No	No	No	Yes
CYP1A2 inhibitor	Yes	Yes	Yes	Yes	Yes	Yes	Yes	Yes	Yes	No
CYP2C19 inhibitor	Yes	Yes	Yes	Yes	Yes	Yes	Yes	Yes	Yes	No
CYP2C9 inhibitor	No	Yes	Yes	Yes	Yes	No	Yes	No	Yes	No
CYP2D6 inhibitor	No	Yes	No	No	Yes	No	No	Yes	No	No
CYP3A4 inhibitor	No	Yes	No	No	Yes	Yes	No	No	No	Yes
log Kp (cm/s)	-5.38	-5.57	-5.14	-5.36	-5.77	-5.95	-4.85	-5.16	-5.07	-6.37
Bioavailability Score	0.55	0.55	0.55	0.55	0.55	0.55	0.55	0.55	0.55	0.55
Synthetic Accessibility	2.74	2.87	2.73	2.76	3.00	2.77	3.17	2.55	3.05	3.29

Table S5: Predicted data of cardiotoxicity of compounds **2a-j**[4]

Compound	Prediction / Potency	Confidence	Applicability domain (AD)	Probabilty Map
2a	Weak or Moderate Potential cardiotoxic (+)	50%	No (Value= 0.24 and limit = 0.26)	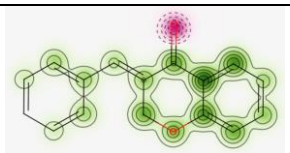
2b	Weak or Moderate Potential cardiotoxic (+)	60%	Yes (Value= 0.26 and limit = 0.26)	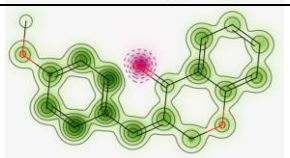
2c	Weak or Moderate Potential cardiotoxic (+)	60%	No (Value= 0.24 and limit = 0.26)	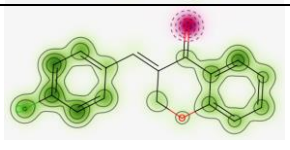
2d	Weak or Moderate Potential cardiotoxic (+)	50%	No (Value= 0.24 and limit = 0.26)	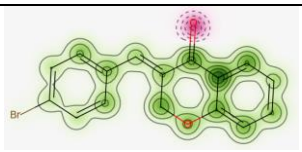

2e	Weak or Moderate Potential cardiotoxic (+)	50%	No (Value= 0.23 and limit = 0.26)	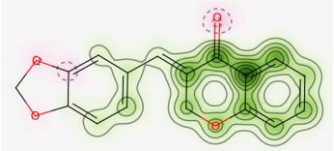
2f	Weak or Moderate Potential cardiotoxic (+)	50%	No (Value= 0.22 and limit = 0.26)	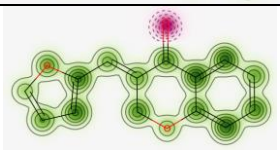
2g	Weak or Moderate Potential cardiotoxic (+)	60%	No (Value= 0.23 and limit = 0.26)	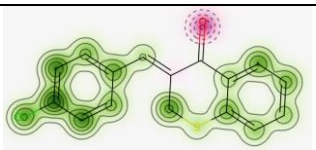
2h	Weak or Moderate Potential cardiotoxic (+)	60%	Yes (Value= 0.27 and limit = 0.26)	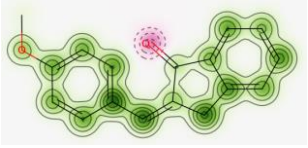
2i	Non-cardiotoxic (-)	60%	No (Value= 0.24 and limit = 0.26)	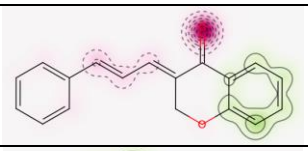
2j	Non-cardiotoxic (-)	60%	No (Value= 0.20 and limit = 0.26)	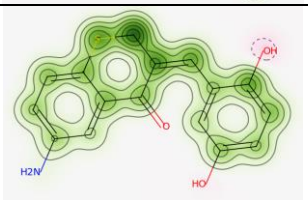

Table S6: Predicted data of toxicity of compounds **2a-j**[5]

	2a	**2b**	**2c**	**2d**	**2e**	**2f**	**2g**	**2h**	**2i**	**2j**
Predicted LD50: mg/kg	2647	2647	2647	2647	2000	2647	2400	1600	2000	400
Prediction accuracy: %	68.07	68.07	68.07	67.38	67.38	67.38	54.26	68.07	67.38	54.26
Organ Toxicity										
Hepatotoxicity (Probability)	0.70	0.68	0.60	0.53	0.76	0.72	0.55	0.56	0.70	0.57
Toxicity end points										
Carcinogenicity	0.55	0.52	0.51	0.56	0.57	0.55	0.69	0.51	0.55	0.54
Immunotoxicity	0.55	0.95	0.85	0.90	0.98	0.88	0.67	0.72	0.77	0.84
Mutagenicity	0.57	0.51	0.50	0.54	0.51	0.51	0.56	0.70	0.57	0.65
Cytotoxicity	0.64	0.73	0.63	0.69	0.88	0.76	0.69	0.69	0.64	0.65
Nuclear receptor signalling pathways										

Aryl hydrocarbon Receptor (AhR)	0.59	0.65	0.62	0.54	0.59	0.59	0.53	0.58	0.59	0.66
Androgen Receptor (AR)	0.93	0.92	0.94	0.95	0.94	0.95	0.98	0.97	0.93	0.95
Androgen Receptor Ligand Binding Domain (AR-LBD)	0.95	0.97	0.91	0.91	0.88	0.95	0.92	0.98	0.95	0.94
Aromatase	0.68	0.78	0.59	0.68	0.92	0.83	0.69	0.82	0.68	0.81
Estrogen Receptor Alpha (ER)	0.52	0.53	0.77	0.78	0.83	0.68	0.72	0.57	0.52	0.57
Estrogen Receptor Ligand Binding Domain (ER-LBD)	0.92	0.88	0.90	0.91	0.98	0.97	0.87	0.83	0.92	0.80
Peroxisome Proliferator Activated Receptor Gamma (PPAR-Gamma)	0.93	0.95	0.77	0.75	0.96	0.93	0.80	0.95	0.93	0.90
Stress response pathways										
Nuclear factor (erythroid-derived 2)-like 2/antioxidant responsive element (nrf2/ARE)	0.88	0.86	0.76	0.76	0.83	0.88	0.64	0.74	0.88	0.82
Heat shock factor response element (HSE)	0.88	0.86	0.76	0.76	0.83	0.88	0.64	0.74	0.88	0.82
Mitochondrial Membrane Potential (MMP)	0.58	0.60	0.52	0.52	0.64	0.61	0.59	0.51	0.58	0.55
Phosphoprotein (Tumor Suppressor) p53	0.65	0.63	0.51	0.52	0.67	0.63	0.62	0.51	0.65	0.69
ATPase family AAA domain containing protein 5 (ATAD5)	0.80	0.72	0.88	0.88	0.82	0.80	0.87	0.84	0.80	0.74
Toxicity Target	Amine Oxidase A	Amine Oxidase A	Amine Oxidase A	Amine Oxidase A	Amine Oxidase A	Amine Oxidase A	-	Amine Oxidase A	Amine Oxidase A	-

Weak Active, **Strong Active**, **Weak Inactive**, **Strong Inactive**

Table S7: Predicted data of toxicity of some FDA approved anti-viral drugs[5]

	Rilpivirine	Dolutegravir	Glecaprevir	Grazoprevir	Paritaprevir
Predicted LD50: mg/kg	2450	1600	68	68	200
Prediction accuracy: %	67.38	54.26	23	54.26	54.26
Organ Toxicity					
Hepatotoxicity (Probability)	0.55	0.76	0.56	0.59	0.51
Toxicity end points					
Carcinogenicity	0.69	0.62	0.58	0.58	0.63
Immunotoxicity	0.94	0.98	0.96	0.99	0.99
Mutagenicity	0.60	0.56	0.64	0.62	0.63
Cytotoxicity	0.76	0.62	0.50	0.54	0.54
Nuclear receptor signalling pathways					
Aryl hydrocarbon Receptor (AhR)	0.66	0.89	0.90	0.87	0.90
Androgen Receptor (AR)	0.99	0.94	0.94	0.92	0.95
Androgen Receptor Ligand Binding Domain (AR-LBD)	0.98	0.97	0.91	0.93	0.93
Aromatase	0.82	0.88	0.83	0.92	0.94
Estrogen Receptor Alpha (ER)	0.61	0.84	0.87	0.88	0.89
Estrogen Receptor Ligand Binding Domain (ER-LBD)	0.95	0.95	0.95	0.97	0.97
Peroxisome Proliferator Activated Receptor Gamma (PPAR-Gamma)	0.98	0.97	0.92	0.85	0.88
Stress response pathways					
Nuclear factor (erythroid-derived 2)-like 2/antioxidant responsive element (nrf2/ARE)	0.96	0.95	0.88	0.88	0.92
Heat shock factor response element (HSE)	0.96	0.95	0.88	0.88	0.92
Mitochondrial Membrane Potential (MMP)	0.81	0.76	0.62	0.61	0.73
Phosphoprotein (Tumor Suppressor) p53	0.84	0.76	0.85	0.85	0.87
ATPase family AAA domain containing protein 5 (ATAD5)	0.83	0.94	0.92	0.95	0.95

References

1. Gaussian 09, Revision D.01, M. J. Frisch, G. W. Trucks, H. B. Schlegel, G. E. Scuseria, M. A. Robb, J. R. Cheeseman, G. Scalmani, V. Barone, B. Mennucci, G. A. Petersson, H. Nakatsuji, M. Caricato, X. Li, H. P. Hratchian, A. F. Izmaylov, J. Bloino, G. Zheng, J. L. Sonnenberg, M. Hada, M. Ehara, K. Toyota, R. Fukuda, J. Hasegawa, M. Ishida, T. Nakajima, Y. Honda, O. Kitao, H. Nakai, T. Vreven, J. A. Montgomery, Jr., J. E. Peralta, F. Ogliaro, M. Bearpark, J. J. Heyd, E. Brothers, K. N. Kudin, V. N. Staroverov, R. Kobayashi, J. Normand, K. Raghavachari, A. Rendell, J. C. Burant, S. S. Iyengar, J.Tomasi, M. Cossi, N. Rega, J. M. Millam, M. Klene, J. E. Knox, J. B. Cross, V. Bakken, C. Adamo, J. Jaramillo, R. Gomperts, R. E. Stratmann, O. Yazyev, A. J. Austin, R. Cammi, C. Pomelli, J. W. Ochterski, R. L. Martin, K. Morokuma, V. G. Zakrzewski, G. A. Voth, P. Salvador, J. J. Dannenberg, S. Dapprich, A. D. Daniels, Ö. Farkas, J. B. Foresman, J. V. Ortiz, J. Cioslowski, and D. J. Fox, Gaussian, Inc., Wallingford CT, 2009.
2. Daina, A.; Michielin, O.; Zoete, V., SwissADME: a free web tool to evaluate pharmacokinetics, drug-likeness and medicinal chemistry friendliness of small molecules, *Scientific Reports*, **2017**, *7*, 42717
3. Sousa; S. F.; Fernandes, P. A.; Ramos, M. J. Protein-ligand docking: current status and future challenges. Proteins. **2006**, *65*, 15-26.
4. http://predherg.labmol.com.br/
5. http://tox.charite.de/protox_II/index.php?site=compound_input